

Fluoride selective chemosensor derived from vitamin B₆ cofactor pyridoxal

Suban K Sahoo^{a,*}, Darshna Sharma^a, Anuradha Moirangthem^b, Anupam Basu^{b,*},
Ashok Kumar S K^c & Umesh D Patil^d

^aDepartment of Applied Chemistry, SV National Institute of Technology (SVNIT), Surat 395 007, Gujarat, India
Email: suban_sahoo@rediffmail.com

^bMolecular Biology and Human Genetics Laboratory, Department of Zoology, The University of Burdwan,
Burdwan 713 104 West Bengal, India
Email: abasu@zoo.buruniv.ac.in

^cSchool of Advanced Sciences, Vellore Institute of Technology University, Vellore 632 014, Tamilnadu, India

^dDepartment of Chemistry, SSVPS's L K Dr P R Ghogrey Science College, Dhule 424 001, Maharashtra, India

An easy-to-prepare and non-cytotoxic Schiff base receptor (**L**) is synthesized by condensation of pyridoxal with aniline. The anion sensing ability of **L** is explored by naked-eye, UV-vis and fluorescence methods. The receptor **L** shows a high selectivity and sensitivity for the sensing of fluoride anion among the other tested competitive anions. The sensor **L** shows both naked-eye detectable color change and significant 'turn-on' fluorescence at 550 nm in the presence of F⁻ with the detection limit as low as 0.4 μM. The fluoride recognition by **L** is supported by ¹H NMR and DFT data. The detection of cytoplasmic fluoride was tested in human cancer cell HeLa through fluorescence imaging.

Keywords: Chemosensors, Anion sensors, Anion recognition, Fluoride sensor, Fluorescent turn-on, Schiff base receptors, Vitamin B₆ cofactor, Pyridoxal

There is continuous growth in the development of highly sensitive and selective chromogenic and fluorogenic chemosensors for the qualitative and quantitative detection of biologically important analytes.^{1,2} Among these analytes, the Hofmeister series of anions are ubiquitous in nature and have a wide range of vital role in biology, medicine, catalysis, environment and industrial raw materials.^{3,4} Fluoride is the smallest anion among the Hofmeister series of anions, and possesses the highest charge density, hydration energy of -366.5 kcal/mol and potentially acts as a hard Lewis base ($pK_a = 3.3$) and strong hydrogen-bond acceptor.⁵ Fluoride is used as an additive in toothpastes because of its important role in dental health and for the treatment of osteoporosis.⁶ Therefore, the United States Environmental Protection Agency (USEPA) mandates a drinking water standard for fluoride of 200 μM and 100 μM to prevent osteofluorosis and dental fluorosis, respectively.⁷ In a recent review, it was demonstrated that while the intake of fluoride in water at about 50 μM can prevent tooth decay, above 250 μM it can cause mottled teeth and bone damage.⁸ In addition, over-exposure to fluoride can lead to acute gastric, kidney and related health problems.⁹⁻¹¹ It should be noted here that fluoride is absorbed easily by the

body, but excreted very slowly. As drinking water is the largest single contributor to daily fluoride intake, the qualitative and quantitative detection of fluoride becomes the focus of considerable interest.

For the detection of fluoride, several methods have been developed, such as the ion-selective electrodes¹², ion chromatography¹³, ¹⁹F NMR analysis¹⁴, reverse-phase HPLC¹⁵, etc. These methods have significant disadvantages of tedious procedure, and need of costlier instruments and trained chemists. Therefore, there is an exponential growth in the development of simple and effective colorimetric and fluorescence chemosensors for the detection of fluoride.¹⁶ Chemosensors possessing polar -NH/-OH/-SH groups as hydrogen bond acceptor, metal complexes, organosilicon-derivatives are extensively studied for the detection of fluoride, but only few of them function in aqueous medium and biological samples.

As a part of our ongoing research on anion recognition and sensing¹⁷⁻²⁰, we have found that the Schiff bases derived using Vitamin B₆ cofactor like pyridoxal and pyridoxal-5-phosphate showed a prominent color change and remarkable 'turn-on' fluorescence for the selective detection of bioactive anions like fluoride and acetate. Herein, we have introduced a simple Schiff base receptor **L** derived by

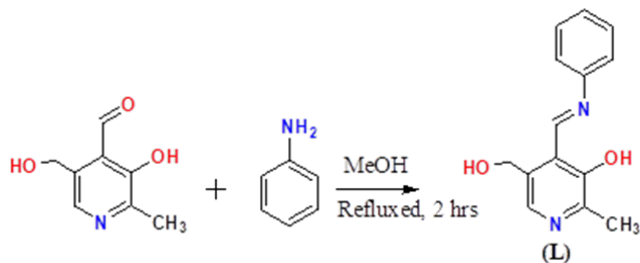
the condensation of pyridoxal and aniline (Scheme 1). The anion sensing ability of **L** was investigated by experimental (naked-eye, UV-vis, fluorescence, ^1H NMR) and DFT methods. Sensor **L** showed fluoride selective colorimetric and turn-on fluorescence in mixed DMSO- H_2O medium. **L** has been successfully applied for the detection of cytoplasmic fluoride in human cancer cell HeLa through fluorescence imaging.

Materials and Methods

All chemicals such as pyridoxal, HCl, aniline and KOH required for the synthesis of receptor **L** were obtained commercially from Acros Organic, India. The spectroscopic grade solvents used for the different experiments were obtained commercially from Merck, India, and were used without further purification. All the anions were used in the form of tetra-*n*-butylammonium (TBA) salts and were purchased from Spectro Chem Pvt. Ltd., India.

Melting points were measured with a digital melting point apparatus (VMP-DS "VEEGO") and are uncorrected. The UV-vis absorption spectra were recorded on a Varian Cary 50 spectrophotometer with a quartz cuvette of 1 cm path length. The fluorescence spectra were recorded on a Horiba FluoroMax-4 spectrometer. ^1H NMR spectra were recorded in DMSO- d_6 on a Bruker Avance II 400 MHz NMR spectrometer, using TMS as an internal standard.

All experiments were conducted in room temperature. Stock solutions of the receptor **L** (1.0×10^{-4} M) and anions (1.0×10^{-3} M) were prepared in DMSO. These solutions were used for all spectroscopic studies after appropriate dilution. The experiments in mixed systems were performed by adding the appropriate amount of doubly distilled water while making the working concentrations of the receptor and anions. For UV-vis absorption titrations, the required amount of the receptor **L** (2 mL, 1.0×10^{-5} M) was taken directly in a cuvette and the spectra were recorded after successive addition of anion (5 μL , 1.0×10^{-3} M) using a micropipette. Similarly, for the fluorescence titration, the spectra of the receptor **L** (2 mL, 5.0×10^{-5} M) were recorded after each incremental addition of F^- (10, 20, 30, 40, 50, 60, 70, 80, 90, 100, 120, 140, 160, 180, 200, 250, 300, 400 and 500 μL , 1.0×10^{-3} M). The sample for the ^1H NMR study was prepared by



Scheme 1

both the anion and receptor in an appropriate ratio. The mixture was made soluble in DMSO- d_6 and then the spectrum was recorded.

Synthesis of **L**

The receptor **L** was synthesised as follows: Pyridoxal hydrochloride (0.5 g, 0.0024 mol) was desalted by adding KOH (0.13 g, 0.0024 mol) in methanolic medium (10 mL). After filtering off KCl, aniline (0.22 g, 0.0024 mol) in 5 ml MeOH was added dropwise into the filtrate at room temperature. Then, the mixture was refluxed for 2 h. A yellow colored precipitate was obtained, which was filtered off, and washed with cold ethanol, followed by ether. The product was recrystallized to give yellow crystals. Yield: 70%; m. pt.: 190 °C; FT-IR (KBr pellet, cm^{-1}): 3098, 2962, 2890, 2831, 2739, 2645, 2361, 1960, 1612, 1582, 1547, 1480, 1450, 1404, 1324, 1288, 1266, 1200, 1072, 1027, 952, 891, 852, 786, 768, 718, 685, 646, 612, 576, 529, 498; ^1H NMR (300 MHz, DMSO- d_6 , Me_4Si , δ , ppm): 14.18 (br, 1H, $-\text{OH}$), 9.27 (s, 1H, $-\text{CH}=\text{N}$), 8.07 (s, 1H, Ar-H), 7.58 (d, $J = 7.83$ Hz, 2H, Ar-H), 7.52 (t, $J = 7.42$ Hz, 2H, Ar-H), 7.41 (t, $J = 7.33$ Hz, 1H, Ar-H), 5.74 (b, Alc- OH), 5.21 (d, $-\text{CH}_2-\text{OH}$), 2.47 (s, $-\text{CH}_3$); LC-MS for $\text{C}_{14}\text{H}_{14}\text{N}_2\text{O}_2$: calc.: 242.27; found: 243.11.

Cytotoxicity assay

The MTT assay was carried out to check the cytotoxic effect of the receptor **L** on HeLa cells. The cells were seeded in a 24-well culture plate with a seeding density of 10×10^4 cells per well in 500 μL complete DMEM media and incubated at 37 °C in a humidified atmosphere with 5% CO_2 . When the cells had reached nearly 60% confluence, the complete media was replaced with serum-free media and incubated with **L** (1.65 mM) for 15 min and F^- (8.7 mM) for nearly 10 min. After incubating with **L** and F^- , the media was replaced with fresh serum-free media, and to it 50 μL of 3-(4,5-dimethylthiazol-2-

yl)-2,5-diphenyltetrazolium bromide, and thiazolyl blue (MTT, 5 mg/mL PBS) were added. At the end of the incubation, DMSO was added to dissolve the insoluble purple formazan product into a colored solution. The absorbance of the converted colored solution was then measured spectrophotometrically at 590 nm.

Live cell imaging

For the live cell imaging of fluoride anions using the receptor **L**, the HeLa cells were first seeded in a 35 mm cell culture dish in DMEM media containing 10% FBS and 1% L-glutamine-penicillin-streptomycin and maintained at 37 °C in a humidified atmosphere with 5% CO₂. After the cells had reached nearly 60% confluence, the complete media was replaced with serum-free media and the cells were incubated with 1.65 mM of **L**. The cells were then washed off to remove any unbound **L** and incubated again with F⁻ (8.7 mM). The cells were observed under the fluorescence microscope using a blue filter (450-490 nm) (Leica DMI6000B). Fluorescence images of the cells were captured through an attached CCD camera using image acquisition software (LAS V4.2). All the images were taken at 20X magnification.

Results and Discussion

UV-vis absorption studies

The receptor **L** was readily synthesized by simple Schiff base condensation of pyridoxal and aniline. The molecular structure of **L** was characterized by various spectral (FTIR, mass and ¹H NMR) data (Supplementary Data, Figs S1-S2). Then, the anion sensing ability of **L** (5.0×10⁻⁵ M, in DMSO) was investigated by naked-eye and UV-vis absorption spectroscopy in the presence of equivalent amounts of different anions (TBA salts of AcO⁻, F⁻, Cl⁻, Br⁻, I⁻, HSO₄⁻ and H₂PO₄⁻, in DMSO). As shown in Fig. 1, the receptor **L** showed a perceptible color change from colorless to dark yellow in the presence of F⁻ anions. No noticeable color change of **L** was observed upon addition of Cl⁻, Br⁻, I⁻, H₂PO₄⁻ and HSO₄⁻ ions, except for AcO⁻ which showed a light yellow coloration. In UV-vis absorption spectroscopy (Fig. 1), the receptor **L** showed a broad absorption between 275 nm and 390 nm due to the multiple types π→π* and n→π* transitions. In presence of F⁻, the receptor showed a new intense peak at 450 nm due to the formation of a receptor-anion complex through

multiple intermolecular hydrogen bonding and/or the deprotonation of the -OH groups of **L**. The host-guest interaction allowed an internal charge transfer (ICT) between the receptor **L** and F⁻, which generated the new intense peak in the visible region responsible for the yellow coloration. Similar to F⁻, the addition of AcO⁻ anions also perturbed the absorption spectrum of **L**, but the intensity of the peak at 450 nm was much lower than that of F⁻. A slight or no significant spectral changes of **L** were observed in the presence of the other anions, viz., Cl⁻, Br⁻, I⁻, H₂PO₄⁻ and HSO₄⁻.

The anion binding ability was estimated by performing the UV-vis absorption titrations of **L** (1.0×10⁻⁵ M) upon stepwise addition of TBAF (tetra-*n*-butylammonium fluoride) and TBAAcO (tetra-*n*-butylammonium acetate) in DMSO. Both the anions showed similar spectral changes with **L**, which indicates the similar recognition modes in solution (Fig. 2 and Supplementary Data, Fig. S3). Upon incremental addition of F⁻/AcO⁻, the intensity of the charge transfer band at 450 nm was concomitantly raised with the formation of an isosbestic point at ~390 nm. The spectroscopic titration data were examined by applying the Benesi-Hildebrand (B-H) equation to calculate the binding constants (*K*) of the receptor-anion complexes.²¹ From the B-H plots (Supplementary Data, Figs S4-S5), the binding constant of **L** for F⁻ (3.12×10⁴ M⁻¹) was found to be higher than that of the AcO⁻ (1.77×10³ M⁻¹). The

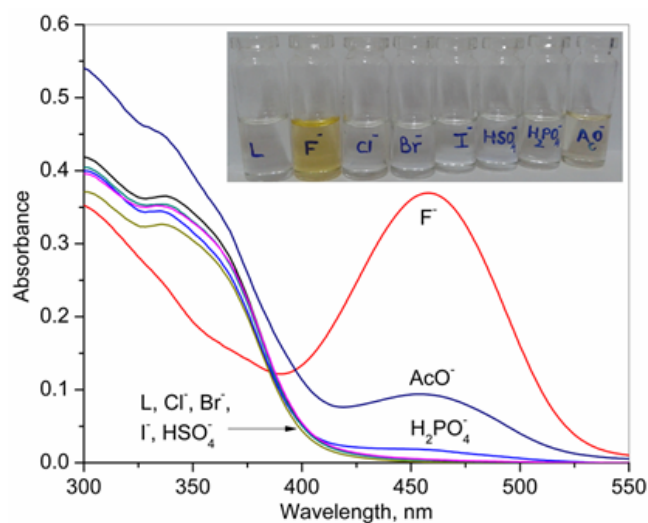


Fig. 1 – UV-vis absorption spectral changes of **L** (5.0×10⁻⁵ M) upon addition of equivalent amounts of different anions (Cl⁻, Br⁻, I⁻, H₂PO₄⁻ and HSO₄⁻) in DMSO.

receptor **L** showed a higher binding affinity towards F^- presumably due to the stronger basicity and H-bond forming ability as compared to AcO^- . Also, the B-H plots indicate the formation of 1:1 host-guest complex, which was further supported from the Job's plot (Fig. 2, Inset).

Fluorescence studies

Anion sensing ability of the receptor **L** (5.0×10^{-5} M, DMSO) was examined by fluorescence spectroscopy (Fig. 3a). The free receptor **L** showed a very weak broad emission between 460-600 nm ($\lambda_{exc} = 435$ nm). The fluorescence of **L** was significantly enhanced at 550 nm in the presence of F^- and AcO^- presumably

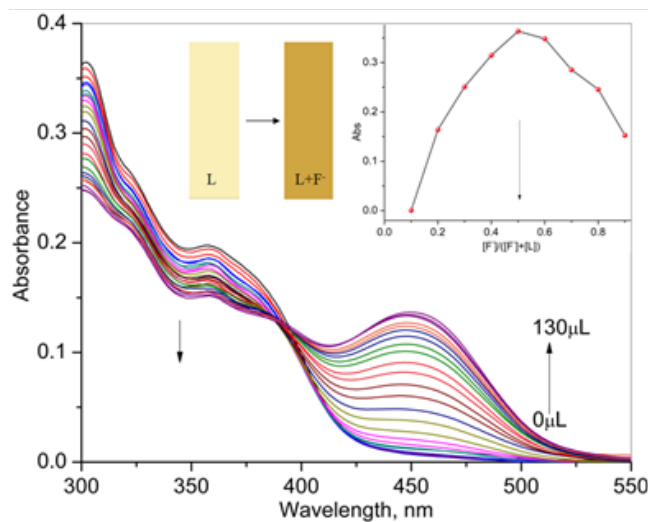


Fig. 2 – Changes in the absorbance spectrum of **L** (1.0×10^{-5} M) upon addition of incremental amounts of TBAF (1.0×10^{-3} M) in DMSO. [Inset shows the color change of test paper strip in the presence of TBAF and the Job's plot].

due to the deprotonation of pyridoxal-OH and the inhibition of excited state intramolecular proton transfer (ESIPT). No significant changes were observed with the other examined anions such as Cl^- , Br^- , I^- , and HSO_4^- , except $H_2PO_4^-$ for which a weak fluorescent enhancement was observed.

It is well known that the recognition and sensing of anions in an aqueous medium is a challenging task because the water molecules can compete with anion for binding sites of the host and hinder the interaction between the receptor and anion. Surprisingly, upon addition of 1% H_2O to the DMSO solution of **L**, the fluorescence selectivity towards fluoride increased remarkably as compared to the other tested anions including AcO^- (Fig. 3b). Also, in the mixed DMSO- H_2O system, the detection of fluoride by **L** was not interfered due to the presence of other competitive anions, viz., Cl^- , Br^- , I^- , AcO^- , $H_2PO_4^-$ and HSO_4^- (Supplementary Data, Fig. S6). Similar fluoride selectivity by **L** was observed in DMSO containing 1% H_2O as shown by absorption spectroscopy (Supplementary Data, Fig. S7).

The limit of detection (LOD) was determined by performing fluorescence titration of **L** with the incremental additions of TBAF in DMSO containing 1% H_2O (Fig. 4). Upon progressive addition of F^- (0–9 equiv.), the fluorescence emission intensity at 550 nm was gradually enhanced. From fluorescence titration data, the detection limit ($3\sigma/S$) of the receptor **L** as a fluorescent 'turn-on' sensor for the analysis of F^- was estimated to be $0.40 \mu M$. The obtained detection limit is much better than the permissible limit of F^- in drinking water. In addition, the detection

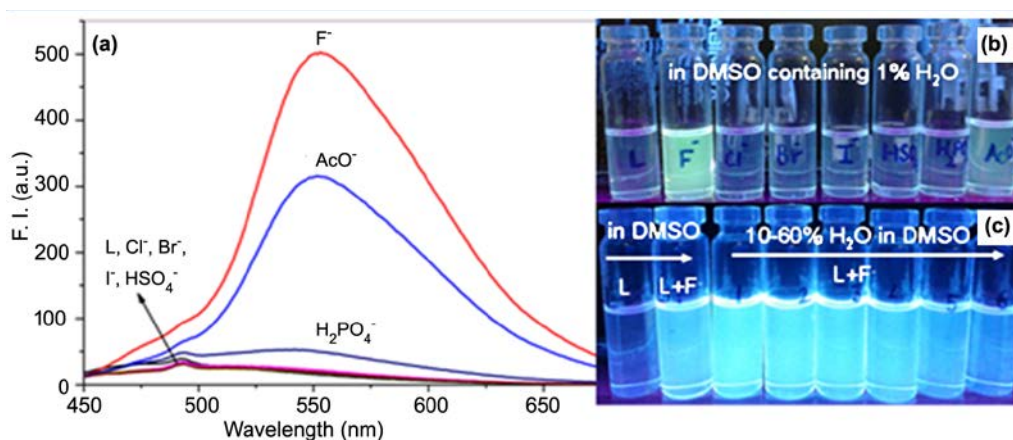


Fig. 3 – (a) Changes in the emission spectrum of **L** (5.0×10^{-5} M) upon addition of equivalent amounts of different anions in DMSO. The change in fluorescence color under UV light (365 nm) in (b) DMSO containing 1% H_2O and (c) **L**+ F^- solutions in DMSO containing varying water content [Water content: 0, 10, 20, 30, 40, 50, 60%].

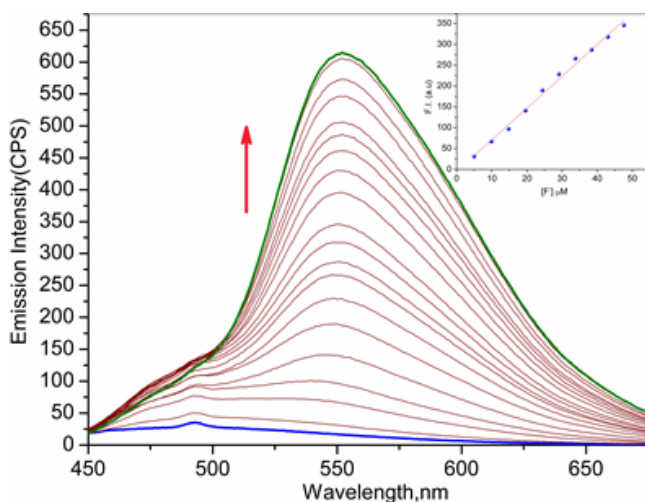


Fig. 4 – Fluorescence titration of **L** (5.0×10^{-5} M) on incremental addition of F^- (10-500 μ L, 1.0×10^{-3} M) in DMSO containing 1% H_2O . [Inset shows the linear curve fitting of fluorescent intensity at 550 nm as a function of concentration of F^-].

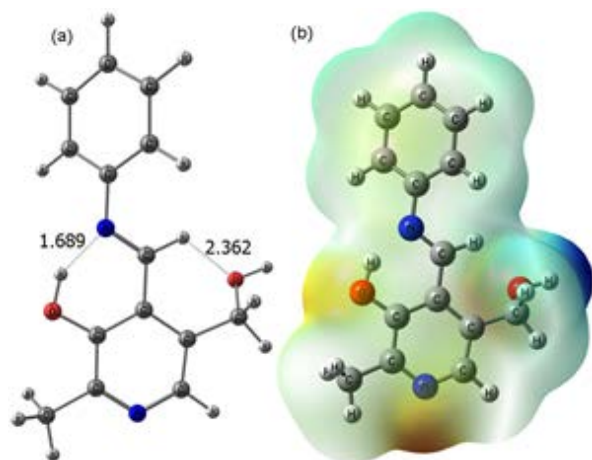


Fig. 5 – Optimized structure of (a) **L** and (b) MEP diagram obtained at B3LYP/6-31G(d,p) level.

of fluoride was examined in DMSO containing various percentages of H_2O (0, 10, 20, 30, 40, 50 and 60%). As shown in Fig. 3c, the turn-on fluorescence of **L** was observed up to water content of 40% in DMSO, which can be visually detected by the color change of **L** under UV light. These results indicate the analytical potential of **L** as a fluorescent ‘turn-on’ sensor for the monitoring and detection of fluoride in real samples.

Anion recognition mechanism

To understand the anion recognition sites and modes, the 3D optimized structure of **L** was first calculated at the B3LYP/6-31G(d,p) level in the gas phase using the computer program Gaussian 09W²²

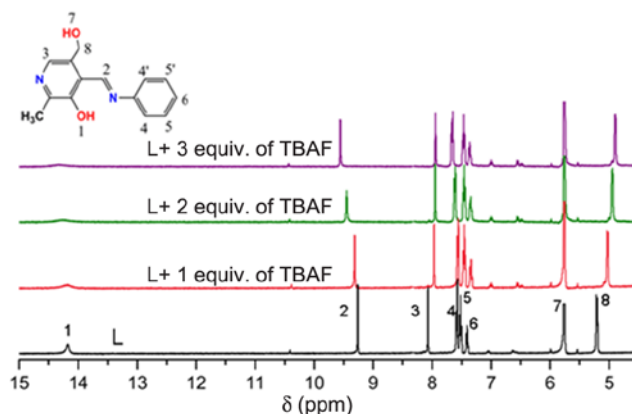


Fig. 6 – 1H NMR spectra of **L** in absence and presence of different equivalents of TBA salts of fluoride and acetate in $DMSO-d_6$.

(Fig. 5a). The enolimine form of **L** was found energetically more stable than the ketoenamine form by 3.26 kcal/mol. The calculated UV-vis spectrum simulated using the TDB3LYP/6-31G(d,p) method gave the maximum absorption at 357 nm and 419 nm respectively for the enolimine and the ketoenamine forms of **L**. The experimental UV-vis absorption of **L** below 400 nm as well as the theoretical results clearly indicate the existence of predominantly an enolimine form of **L**. Then, the possible sites of **L** for the anion recognition were identified from Mulliken’s atomic charge analysis. The aromatic-OH, alcoholic-OH and imine-H protons possess the maximum positive Mulliken’s atomic charges of 0.356, 0.311 and 0.118 to make interaction with an incoming anion possible, which is further supported by the analysis of molecular electrostatic potential (MEP) map of **L** (Fig. 5b, where the most positive and negative regions are respectively shown in blue and red color).

Anion recognition by **L** was further examined by 1H NMR titration of **L** with different equivalents of TBAF in $DMSO-d_6$ (Fig. 6 and for the upfield region see Supplementary Data, Fig. S8). The receptor showed a singlet due to the aromatic-OH, alcoholic-OH and imine-H protons at 14.18 ppm, 5.74 ppm and 9.27 ppm, respectively. The downfield peak due to $-OH$ proton indicates the presence of intramolecular hydrogen bonds (Fig. 5a). Addition of varying equivalents of F^- resulted in the downfield shift of the aromatic-OH and imine-H signals. Also, the aromatic-OH proton signal was broadened along with an appreciable decrease in intensity due to elongation of the O-H bond length followed by deprotonation upon interaction with F^- . Similarly, a slight downfield shift of alcoholic-OH proton signal was observed. Other

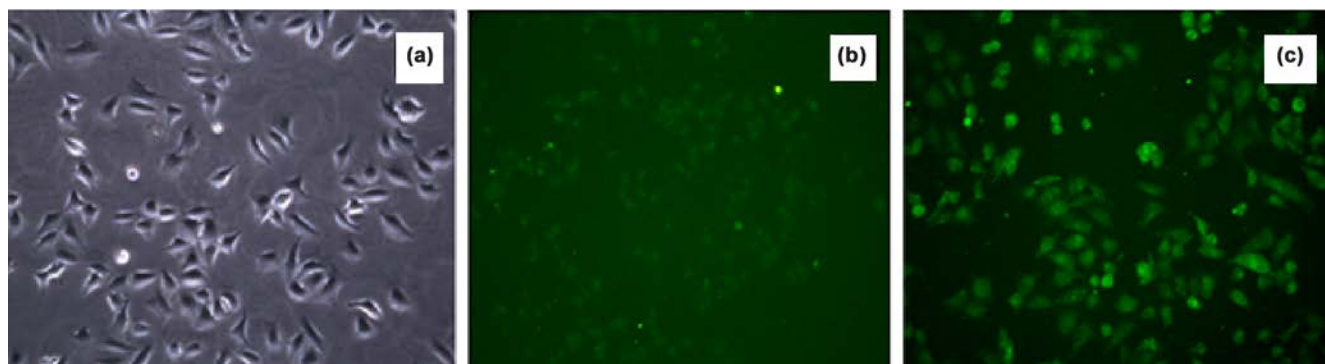


Fig. 7 – (a) Phase contrast image of the control cells, (b) Fluorescence image of the cells after incubating with **L** (1.65 mM) only, as observed through excitation filter 450-490 nm, and, (c) Fluorescence image of the cells after incubating with **L** (1.65 mM) and F^- (8.73 mM), as observed through excitation filter 450-490 nm. [All the images were taken at 20X magnification through an attached CCD camera using image acquisition software, LAS V4.2].

signals due to aromatic-H and $-CH_2-$ protons were shifted upfield. The characteristic bifluoride (HF_2^-) peak supporting the deprotonation mechanism at ~ 16.0 ppm was not observed even after the addition of 3.0 equiv. of TBAF.²³ These results clearly show that the receptor **L** recognized fluoride by utilizing the aromatic-OH, alcoholic-OH and imine-H protons, and the deprotonation of aromatic-OH occurred at a higher equivalent of fluoride.

For additional evidence on the anion recognition modes of **L**, the naked-eye detectable color and spectral changes of the receptor **L** (5.0×10^{-5} M, in DMSO) were investigated at varying pH in the absence and presence of TBAF (Supplementary Data, Figs S9-S10). The receptor **L** alone in DMSO (pH = 9.25) showed a detectable color change under daylight and UV light. Also, a new intense absorption band was seen at 450 nm only when the pH was increased to 10.75 using 0.1 N KOH. Similar changes of **L** were observed in the presence of an equivalent amount of TBAF. Addition of TBAF to a solution of **L** increased the pH of the medium from 9.25 to 11.22. This result clearly shows that here the fluoride ion acts as a strong base and abstracted/elongated the most acidic protons present in the receptor. Thus, the results obtained from 1H NMR and the effect of pH study, it can be concluded that first the aromatic $-OH$, alcoholic $-OH$ and imine-H protons of the receptor **L** form intermolecular hydrogen bond with fluoride anion to form the host-guest complex and then later, the most acidic aromatic-OH undergoes a partial deprotonation process.

Reversibility of **L** (2 mL in DMSO, 1.0×10^{-5} M) was tested for the sensing of TBAF (1.0×10^{-4} M) and TBAAcO (1.0×10^{-4} M) by addition of $CaCl_2$ solution (1.0×10^{-4} M). As shown in Fig. S11 (Supplementary Data), the color and spectral changes of **L** induced by F^- and AcO^- were reversed in the presence of $CaCl_2$. This interesting colorimetric and spectral behavior changes of **L** in the presence of F^-/AcO^- and Ca^{2+} also allowed us to construct an INHIBIT type molecular logic gate.²⁴

Cytotoxicity assay and live cell imaging

The MTT assay was carried out to check the cytotoxic effect of the receptor **L** in the intracellular detection of fluoride anions (Supplementary Data, Fig. S12). From the MTT assay, it was observed that the receptor **L** and F^- with concentrations of 1.65 mM and 8.73 mM, respectively did not have any remarkable cytotoxic effect. Thus, the receptor **L** can be used for the intracellular detection of fluoride in live cancer cell through bioimaging technique. The non-cytotoxic nature of **L** at lower concentration encouraged us to examine its *in vitro* ability to detect intracellular fluoride in the cervical cancer HeLa cell line by the fluorescence imaging technique. No fluorescence was observed when the cells were incubated with F^- alone (8.73 mM). A slight fluorescence from the cells was observed when the cells were incubated with the receptor **L** alone (Fig. 7b). A surge of increase in the fluorescence was observed from the cells when the receptor **L** (1.65 mM) was incubated with F^- (8.73 mM F^-) (Fig. 7c).

Conclusions

In conclusion, we have introduced a simple and easy-to-prepare fluorescent ‘turn-on’ sensor **L** by combining the vitamin B₆ cofactor pyridoxal with aniline for the selective detection of fluoride anions in the mixed DMSO-H₂O system. Sensor **L** showed turn-on fluorescence for fluoride under a competitive environment with the detection limit as low as 0.40 μM. Sensor **L** showed no cytotoxic effects in live HeLa cells when incubated at 1.65 mM or lower concentrations. Also, sensor **L** was successfully applied for the intracellular detection of fluoride in live cancer cell through bio-imaging technique.

Supplementary data

Supplementary data associated with this article are available in the electronic form at [http://www.niscair.res.in/jinfo/ijca/IJCA_57A\(05\)619-625_SupplData.pdf](http://www.niscair.res.in/jinfo/ijca/IJCA_57A(05)619-625_SupplData.pdf).

References

- 1 Lehn J-M, *Supramolecular Chemistry*, (VCH, Weinheim) 1995.
- 2 Duke R M, Veale E, Pfeffer F M, Kruger P E & Gunnlaugsson T, *Chem Soc Rev* 39 (2010) 3936.
- 3 *Supramolecular Chemistry of Anions*, edited by A Bianchi, K Bowman-James, E Garcia-Espana, (Wiley-VCH, New York, USA) 1997.
- 4 Sessler J L, Gale P A & W-S Cho, in *Anion Receptor Chemistry*, edited by J F Stoddart, Monographs in Supramolecular Chemistry, (Royal Society of Chemistry, Cambridge, UK) 2006.
- 5 Evans N H & Beer P D, *Angew Chem Int Ed*, 53 (2014) 11716.
- 6 Foulkes R G, *Fluoride*, 40 (2007) 229.
- 7 Fawell J, Bailey K, Chilton J, Dahi E, Fewtrell L & Magara Y, *Fluoride in Drinking Water*, WHO Drinking-Water Quality Series, (IWA Publishing, London, UK) 2006.
- 8 Harrison P T, *J Fluorine Chem*, 126 (2005) 1448.
- 9 Michigami Y, Kuroda Y, Ueda K & Yamamoto Y, *Anal Chim Acta*, 274 (1993) 299.
- 10 Kumar M & Puri A, *Indian J Occup Environ Med*, 16 (2012) 40.
- 11 Chinoy J N, *Indian J Environ Toxicol*, 1 (1991) 17.
- 12 Frant M S & Ross J W, *Science*, 154 (1966) 1553.
- 13 Lefler J E & Ivey M M, *J Chromatogr Sci*, 49 (2011) 582.
- 14 Konieczka P, Zygmunt B & Namiesnik J, *Bull Environ Contam Toxicol*, 64 (2000) 794.
- 15 Kibbey C E & Meyerhoff M E, *Anal Chem*, 65 (1993) 2189.
- 16 Zhou Y, Zhang J F & Yoon J, *Chem Rev*, 114 (2014) 5511.
- 17 Sharma D, Mistry A R, Bera R K & Sahoo S K, *Supramolecular Chem*, 25 (2013) 212.
- 18 Sharma D, Moirangthem A, Sahoo S K, Basu A, Roy S M, Pati R K, Ashok Kumar SK, Nandre J P & Patil U D, *RSC Adv*, 4 (2014) 41446.
- 19 Sharma D, S Sahoo K, Chaudhary S, Bera R K & Callan J F, *Analyst*, 138 (2013) 3646.
- 20 Sharma D, Ashok Kumar S K & Sahoo S K, *Tetrahedron Lett*, 55 (2014) 927.
- 21 Benesi H A & Hildebrand J H, *J Am Chem Soc*, 71 (1949) 2703.
- 22 *Gaussian 09W, Rev. A 1*, (Gaussian, Inc, Wallingford CT) 2009.
- 23 Saravan Kumar S, Bothra S, Sahoo S K & Ashok Kumar S K, *J Fluorine Chem* 164 (2014) 51.
- 24 Fegade U A, Sahoo S K, Singh A, Singh N, Attarde S B & Kuwar A S, *Anal Chim Acta* 872 (2015) 63.